

## **Comparative Aerodynamic Efficiency Analysis of a Conventional and Slotted Wing using ANSYS Fluent Simulation**

**Hasan.f.AL-Dabaagh**

**Department of Aeronautical Technical Engineering, Technical Engineering  
College of Najaf, Al-Furat Al-Awsat Technical University, Iraq**

### **Abstract:**

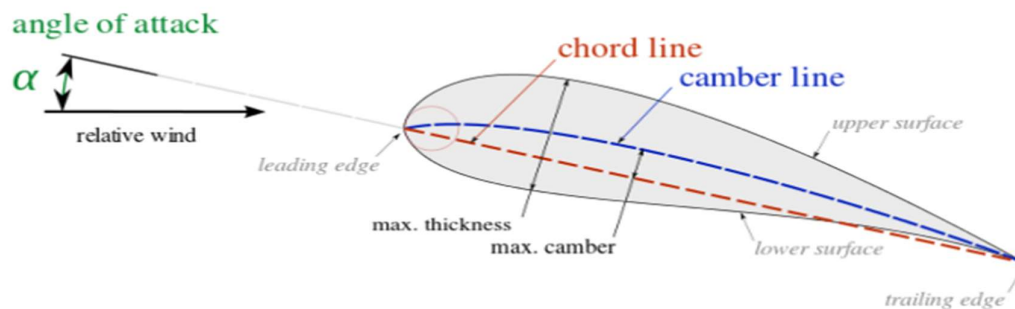
This study investigates the aerodynamic efficiency of two wing designs: a conventional solid wing and a slotted wing with a longitudinal gap. Computational simulations were conducted using ANSYS Fluent to evaluate and compare the aerodynamic performance of both configurations. The slotted wing design is hypothesized to enhance airflow dynamics, potentially reducing drag and increasing lift. The results of the simulation are analyzed based on key performance parameters such as lift-to-drag ratio, pressure distribution, and airflow patterns. The findings aim to provide insights into the benefits and limitations of the slotted wing design for improving aerodynamic efficiency in various applications

### **1.Introduction**

The formation and manufacture of aircraft wings demand Attention to many unique structural requirements. As the wing design plays a high role in the lifting process, as placing a slit at the beginning of the wing section is a new design in the world of aircraft and during this research the comparison with a normal wing that does not contain this slit and through the results it was shown that there is an improvement in speed and pressure reduction. With an increase in the ability to maneuver. We know two basic methods of model analysis, which are numerical analysis and experimental form analysis. The experimental model analysis deals with data input measurements through which a mathematical model is derived. This paper is mainly concerned with numerical conditional analysis. The construction of the wing is similar in most modern aircraft. There will be many constraints and assumptions throughout the analysis. Finally, the structural analysis The data of the distribution of speeds and pressures are obtained through the analysis from end to end Transient structural analysis, which is a plan for improvement and improvement of the design of the aircraft for the future.

### **2. AIRFOIL TERMINOLOGY AND DEFINITIONS**

**2.1 AIRFOIL** In the airfoil profile, the forward point is called the leading edge and the rearward point is called the trailing edge. The straight line connecting the leading and trailing edges is called the chord line of the airfoil. The distance from the leading edge to the trailing edge measured along the chord line is designated as a chord ( $c$ ). The mean camber line is the locus of points midway between the lower surface and upper surface when measured normal to the mean camber line itself. The camber is the maximum distance between the mean camber line and the chordline, measured normal to the chord line. The thickness is the distance between the upper and lower surfaces also measured normal to the chord line. The shape of the airfoil at the leading edge is usually circular, with a leading-edge radius of  $0.02c$ , where  $c$  is the chord length. The upper and lower surfaces are also known as suction and pressure surface respectively.



**2.2 AIRFOIL CLASSIFICATION** The Network of Aquaculture Centers in Asia-Pacific, airfoil series, the 4-digit, 5-digit, and the updated 4-/5- digit, were generated using analytical equations and analogies that described the curvature of the airfoil's mean-line (geometric centerline) as well as the section's thickness distribution along the length. Also, the families, which included the 6-Series, were more complex shapes which were derived using theoretical methods.

**(I) NACA Four-Digit Series:** The family of airfoils which was curated by utilizing this approach was called the NACA Four-Digit Series. Here in, the maximum camber in the percentage of the chord (airfoil length) is given by the first digit, the second indicates the position of the maximum camber and lastly, the maximum thickness of the airfoil in the percentage of the chord is provided by the last two numbers. For example, the NACA 2415 airfoil has a maximum thickness of 15% with a camber of

2% located at 40% chord from the airfoil leading edge (or  $0.4c$ ). Using these values, one can compute the coordinates of the entire airfoil using specific equations.

**(II)NACA Five-Digit Series:** The NACA Five-Digit Series and the Four-Digit Series are quite similar as they use the same thickness forms, but the mean camber line is defined differently and the naming convention is a bit more complex. The design lift coefficient ( $c_L$ ) is given by the first digit, when multiplied by  $3/2$ , yields it in tenths. The next two digits, when divided by 2, give the position of the maximum camber in tenths of the chord. The final two digits again indicate the maximum thickness in a percentage of chord. Taking an example, the NACA 24013 has a peak thickness of 13%, a design lift coefficient of 0.3, and the maximum camber located 20% behind the leading edge. At present, the resources available for computation allow the designers to design and optimize the airfoils specifically tailored to a particular application.

**3. MATERIAL SELECTION** The metals used in the aircraft manufacturing industry include steel, aluminum, titanium and their alloys. In this project two materials are used, they are Aluminium alloy and titanium alloy, both materials have some characteristics which are best suited for wing design.

**4. WING DESIGN PROCEDURE** The amount of lift produced by an airfoil depends upon many factors. They are angle of attack, the lift devices used (like flaps), the density of air, the area of wing, the shape of wing, the speed at which the wing is travelling. Some Factors affecting wing size they are cruise drag, stall speed, take-off and landing distance. The first step is to get the airfoil shape in the CATIA workbench. As we are considering that wing is designed with only one airfoil throughout, it has to be scaled down accordingly to get the required shape of a wing profile.

**4.1 SELECTION OF AIRFOIL** Beforehand the scheme plans underway, values for several constraints must be selected. These comprise the airfoil as, in numerous generations, it is the core of the aircraft. Correspondingly, the airfoil upsets the voyage quickness, take-off, and landing stage spaces, cubicle speed, management abilities, and total aerodynamic efficacy through all stages of voyage. BOEING BACXXX airfoil is being used in Boeing 747-400 and the design has a high lift characteristic in subsonic speed, and thus it is very suitable for the transport aircraft

of Boeing 747-400. Therefore, for wing Skelton structure we use BOEING BACXXX airfoil coordinates.

**4.2 WING COMPONENT DESIGN** The physical structure modelled in this work is an aircraft wing of airfoil cross section BOEING BACXXX. Its dimensions are that of a research subsonic aircraft wing. It is made of an aluminum alloy (1st case) and titanium alloy (2nd case) structure.

Since there are several limitations and due to the wing structure complexity and tremendously laborious if not challenging to convey out, the geometry of the exemplary is streamlined by declining the scale of the wing and omitting numbers of struts as they do not underwrite in contradiction of bending. This can be finished since collapsing on the membrane was not shaped. Moreover, this wing component design is made up of a 1:4 ratio since there are limitations that the software cannot solve the design problem. Thus, the wing structure design specifications are made purposely for this research paper as follows

Wing Span		4500mm
Chord Length		1000mm
Airfoil		BOEING BACXXX
Taper Ratio		1
Sweep Angle		0°
Ribs Design	Root and Tip Thickness	40mm
	Other Ribs	20mm
Spars	Length	4500mm
	Thickness	60mm

**Table 1: Wing component design specification.**

**4.3 Experimental Studies of Flow Separation of the NACA 2412 Airfoil at Low Speeds** Wind tunnel tests have been conducted on an NACA 2412 airfoil section at Reynolds number of  $2.2 \times 10^6$  and Mach number of 0.13. Detailed measurements of flow fields associated with turbulent boundary layers have been obtained at angles of attack of 12.4 degrees, 14.4 degrees, and 16.4 degrees. Pre- and post-separated velocity and pressure survey results over the airfoil and in the



associated wake are presented. Extensive force, pressure, tuft survey, hot-film survey, local skin friction, and boundary layer data are also included. Pressure distributions and separation point locations show good agreement with theory for the two layer angles of attack. Boundary layer displacement thickness, momentum thickness, and shape factor agree well with theory up to the point of separation. There is considerable disparity between extent of flow reversal in the wake as measured by pressure and hot-film probes. The difference is attributed to the intermittent nature of the flow reversal.

**NACA 2412**

<b>1.0000</b>	<b>0.0013</b>
<b>0.9500</b>	<b>0.0114</b>
<b>0.9000</b>	<b>0.0208</b>
<b>0.8000</b>	<b>0.0375</b>
<b>0.7000</b>	<b>0.0518</b>
<b>0.6000</b>	<b>0.0636</b>
<b>0.5000</b>	<b>0.0724</b>
<b>0.4000</b>	<b>0.0780</b>
<b>0.3000</b>	<b>0.0788</b>
<b>0.2500</b>	<b>0.0767</b>
<b>0.2000</b>	<b>0.0726</b>
<b>0.1500</b>	<b>0.0661</b>
<b>0.1000</b>	<b>0.0563</b>
<b>0.0750</b>	<b>0.0496</b>
<b>0.0500</b>	<b>0.0413</b>
<b>0.0250</b>	<b>0.0299</b>
<b>0.0125</b>	<b>0.0215</b>
<b>0.0000</b>	<b>0.0000</b>
<b>0.0125</b>	<b>-0.0165</b>
<b>0.0250</b>	<b>-0.0227</b>
<b>0.0500</b>	<b>-0.0301</b>
<b>0.0750</b>	<b>-0.0346</b>
<b>0.1000</b>	<b>-0.0375</b>
<b>0.1500</b>	<b>-0.0410</b>
<b>0.2000</b>	<b>-0.0423</b>
<b>0.2500</b>	<b>-0.0422</b>
<b>0.3000</b>	<b>-0.0412</b>
<b>0.4000</b>	<b>-0.0380</b>
<b>0.5000</b>	<b>-0.0334</b>
<b>0.6000</b>	<b>-0.0276</b>
<b>0.7000</b>	<b>-0.0214</b>
<b>0.8000</b>	<b>-0.0150</b>
<b>0.9000</b>	<b>-0.0082</b>
<b>0.9500</b>	<b>-0.0048</b>
<b>1.0000</b>	<b>-0.0013</b>

**Table 1: NACA 2412**

### 5. wing drawn

The wing was drawn according to the Naca one, which is 2412, and a normal wing was drawn with a wing containing a slit, and they will be compared.

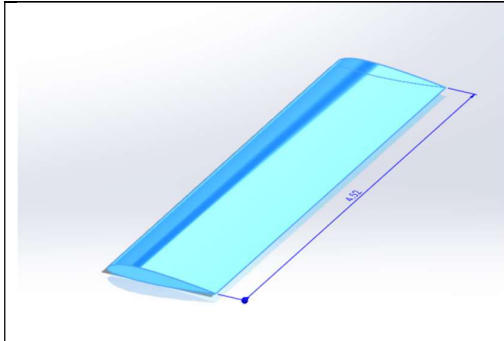


**Figure 1: Standard wing**

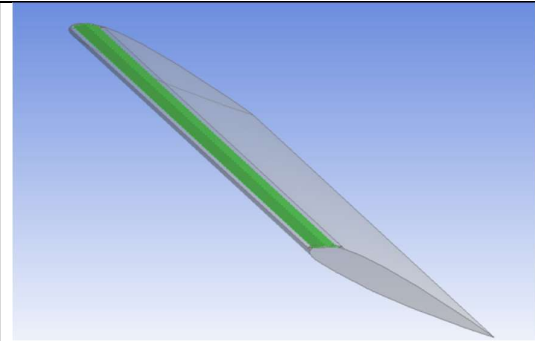
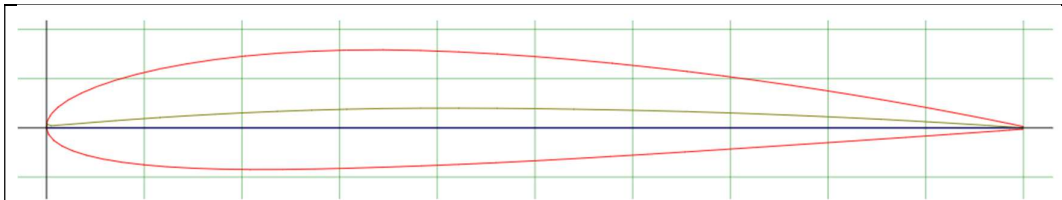


**Figure 2: wing with slit**



**Naca 2412**

### 6. FINITE ELEMENT MESHING AND BOUNDARY CONDITIONS

**Generating** a mesh is one of the most critical steps in FEM for obtaining reasonable results. Many types of, 2D and 3D, elements can be used. Figure illustrates some mesh elements. The type of elements chosen depends on the type of geometry and the nature of the analysis. Each element has an ideal shape and due to complex geometries, the element has to be deformed so that it fits. This is referred to as mesh skewness and the bigger it is the less accurate approximations are. Increasing the number of elements solve the issue of overly skewed elements.



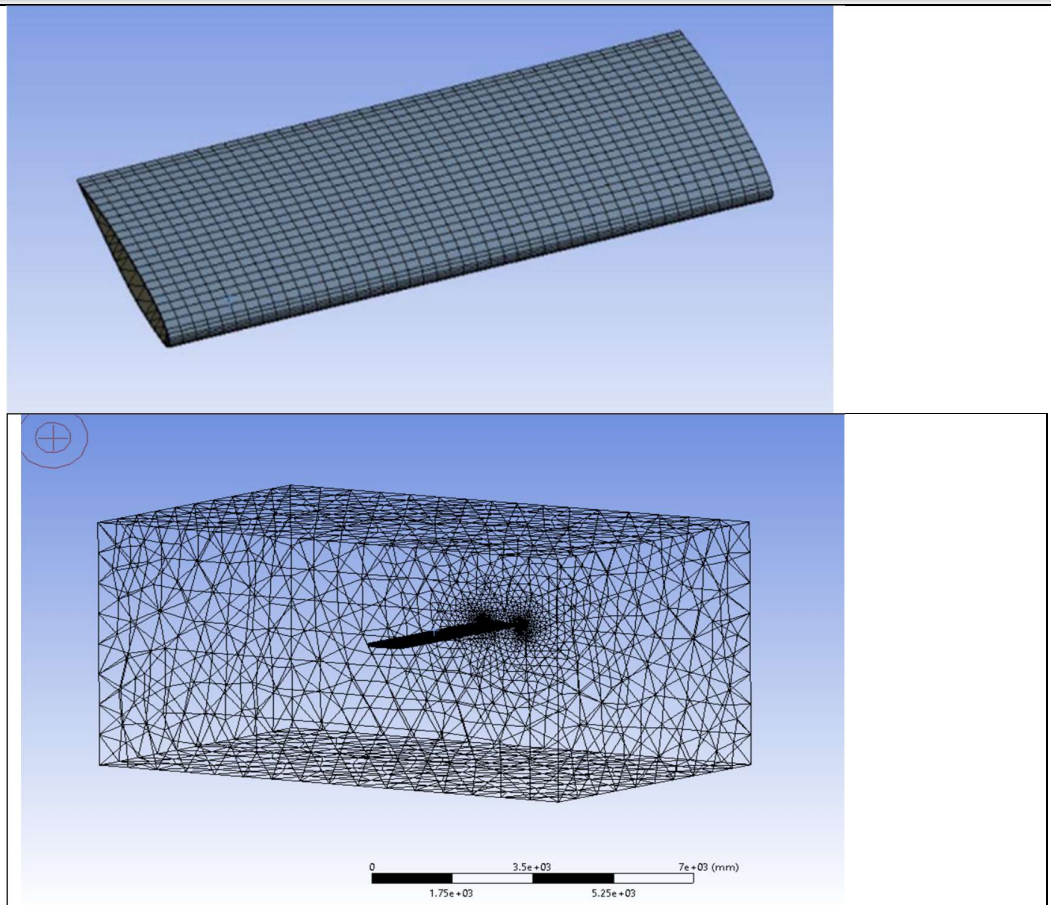


**Figure 3: Meshed wing structure**

## 7. fluid flow analysis

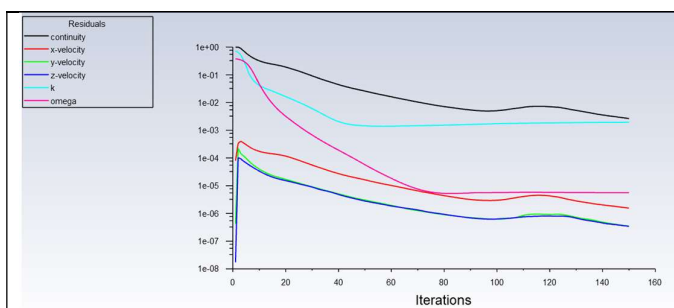


**Figure 4: Standard wing(iteration)**

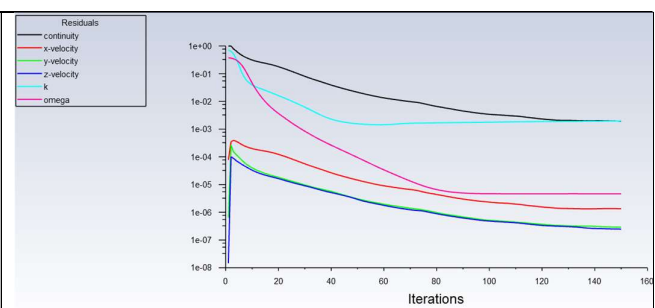


**Figure 5: wing with slit(iteration)**

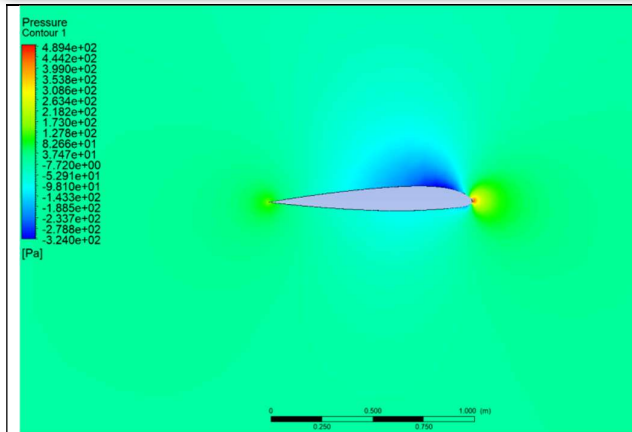


Figure 6: Standard wing (pressure contour)

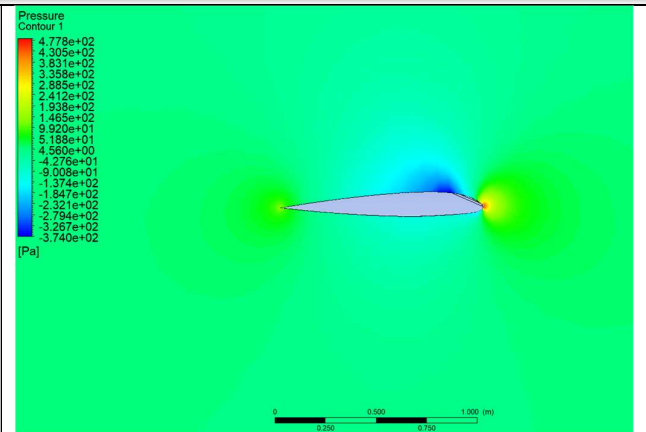


Figure 7: wing with slit (pressure contour)

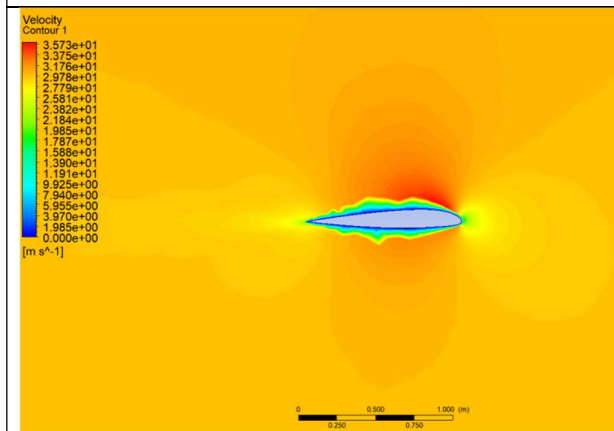


Figure 8: Standard wing (velocity contour)

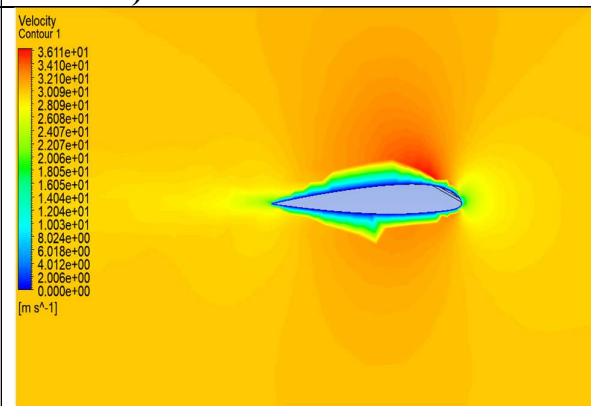


Figure 9: wing with slit (velocity contour)

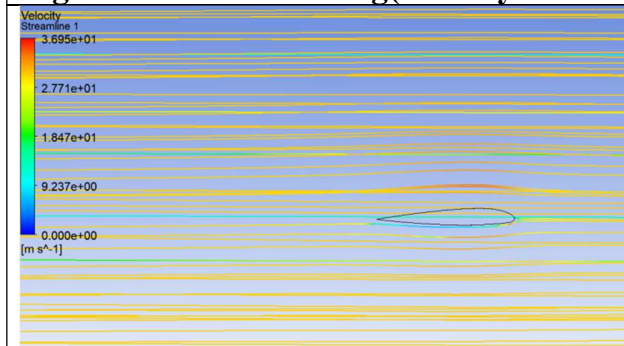


Figure 10: Standard wing (velocity streamline)

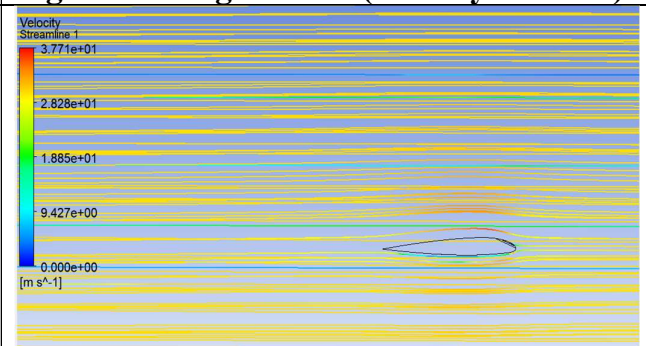
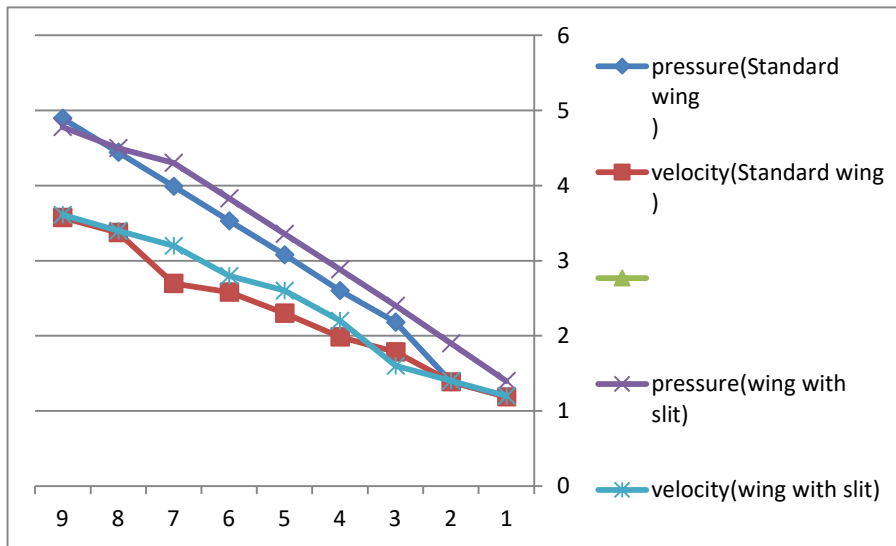


Figure 11: wing with slit (velocity streamline)



pressure (Standard wing)	velocity (Standard wing)	pressure (wing with slit)	velocity (wing with slit)
1.19	1.19	1.4	1.2
1.39	1.39	1.9	1.4
2.18	1.787	2.4	1.6
2.6	1.985	2.881	2.2
3.08	2.3	3.358	2.6
3.53	2.58	3.831	2.8
3.99	2.7	4.305	3.2
4.442	3.375	4.5	3.4
4.894	3.573	4.778	3.611



## 8. Conclusion

Through the results and comparison between the regular wing and the split wing that was done on the Naca type 2412 time during the results it was shown that the wing that contains a split is better than the regular wing in terms of increasing the speed and reducing the pressure distribution through the simulation program. In future studies, the split can be enlarged in order to increase the air flow and increase the flying speed.



## 9. REFERENCES

- [1] Zhang, X., Zhao, Y., & Si, F. (2018). Analysis of wing flexure deformation based on ANSYS. 2018 IEEE/ION Position, Location and Navigation Symposium, PLANS 2018 - Proceedings, 190–196. <https://doi.org/10.1109/PLANS.2018.8373381>. Clerk Maxwell, A Treatise on Electricity and Magnetism, 3rd ed., vol.
- [2] Oxford: Clarendon, 1892, pp.68–73. 2. Obert, E. (2009). Aerodynamic Design of Transport Aircraft. Amsterdam: IOS Press, Delft University Press.
- [3] Vani, P. S., Reddy, D. V. R., Prasad, B. S., & Shekar, K. C. (2014). Design and Analysis of A320 Wing using E-Glass Epoxy Composite. International Journal of Engineering Research & Technology, 3(11), 536–539. Nicole, “Title of paper with the only first word capitalized,” J. Name Stand. Abbrev., in press.
- [4] Raymer, D. P. (1992). Aircraft Design: A Conceptual Approach (Second Edi). Washington, DC: American Institute of Aeronautics and Astronautics, Inc.
- [5] Karukana. (2013). Study of Flow Field over Fabricated Airfoil Models of NACA 23015 with its Kline-Fogelman Variant. Advances in Aerospace Science and Application, 3(2), 95–100.
6. Anderson, J. D. (2012). Introduction to Flight (7th Edition). McGrawHill. [6] A M H Abdul Jalil, W Kuntjoro and J Mahmud 2012 Wing structure static analysis using super Element, Procedia Engineering. 41, 1600 – 1606.
- [7] T V Baughn and P F Packman 1986 Finite element analysis of an ultra-light aircraft, Journal of Aircraft. 23, 82- 86.
- [8] Yuvraj S R and Subramanyam P 2015 Design and analysis of Wing of an ultra-light Aircraft International journal of innovative research in science, engineering and technology. 4, 78-85.